

Speed Control of PMSM with High Step-Up Dual Switch Solar Converter



Pramod Gollapelli, Gopala Venu Madhav

Abstract: For PVA renewable source the output voltage is fluctuating as the solar irradiation is variable with respect to time. In conventional methods to control the DC voltage output of the PVA DC-DC booster converters are used. These converters don't have high gain and also the ripple of the DC output voltage is high. The conventional PWM DC-DC booster converter is replaced with a feedback controlled dual switch converter for better control of output DC voltage with higher gain and reduced ripple. In this paper, the output of the dual switch converter is fed to controlled six switch inverter running a permanent magnet synchronous motor. The motor is controlled with a reference speed control technique for change in variable speed and torque operations. The input voltage of the converter is also made variable with respect to time with change in solar irradiation; the response of the proposed converter is good even for this condition. MATLAB/Simulink is used to design all the modules of the proposed work.

Index Terms: Boost Converter, Dual Switch Converter, PMSM, PVA (Photo Voltaic Array), Speed Control.

I. INTRODUCTION

IN recent years there is a huge development in renewable energy generation with different types of sources. The most flexible and easy to install renewable source is PVA (Photo voltaic Array) [1] which is static device generating power from solar irradiation. The solar panel (PVA) can be installed in any place either urban or rural area with human presence unlike wind farms it doesn't generate any vibrations or disturbances in the environment. However, the power generated by the solar panels is very much less as compared to wind farms with dynamic machines. There are many ongoing researches for improvement of efficiency [2] of PVAs. For a general consideration the power output of a single panel of 1m² the power generated is around 200W. The major advantages of solar panels are low maintenance and less complicated control structure. The major disadvantage of solar panel power generation is it generates fluctuating voltage with variation of solar

irradiation. When the output DC voltage [2] of the solar panel changes the AC output voltage from the inverter also changes which may damage the load or grid connected to it. It is very keen to maintain the DC voltage output of the solar panel at a constant value so as to maintain the AC voltage output of the inverter constant.

This is done by connecting a DC-DC boost converter [3] which controls the output voltage with a feedback control unit. In conventional ways the output voltage of the DC-DC boost converter is controlled by Maximum Power Point Tracking (MPPT) algorithm. The MPPT takes feedback of PVA voltage and current and then controls the duty ratio with respect to change in voltage and current of PVA by variation of solar irradiation. In this paper the conventional MPPT [3] controller with DC-DC boost converter is replaced with a higher efficient and more stable DC-DC converter topology with voltage orient feedback control of the converter. The proposed circuit is dual switch high step up converter with voltage multiplier and coupled inductor. The constant DC output voltage [2] of the proposed converter is fed to six switch inverter operating a PMSM (Permanent magnet synchronous motor). A speed control structure is integrated to the inverter so as to control the speed of the motor. The below is the complete system modeling with PVA, high step up dual switch converter and PMSM motor drive unit.

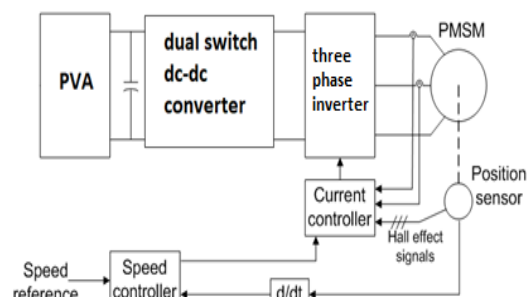


Fig. 1: Block diagram of PVA connected PMSM drive.

The PVA connected to the dual switch converter has 70 cells in series with each cell voltage at 0.42V. The complete output voltage of PVA is 30V. And the number of parallel cells connected to the PVA is 7333 with 10mA current output of each cell, where the complete output current of the PVA is 73.33 amps. The power output of the PVA is given as $P_{pv} = 70 \times 0.42 \times 7333 \times 0.01 = 2.15kW$(1)

Revised Manuscript Received on October 30, 2019.

* Correspondence Author

Pramod Gollapelli*, PG Scholar, Department of EEE, Anurag Group of Institutions, Venkatapur, Ghatkesar, India.

Gopala Venu Madhav, Department of EEE, Anurag Group of Institutions, Venkatapur, Ghatkesar, India.

© The Authors. Published by Blue Eyes Intelligence Engineering and Sciences Publication (BEIESP). This is an open access article under the CC BY-NC-ND license (<http://creativecommons.org/licenses/by-nc-nd/4.0/>)

II. DUAL SWITCH CONVERTER TOPOLOGY

The proposed dual switch converter has a coupled inductor to ensure large storage of charge for high output voltage. The two switches (MOSFETs) connected in the topology operate simultaneously at a high frequency of 50kHz [4]. The duty ratio of the of the converter is controlled by a voltage-oriented feedback loop control, which controls the duty ratio of the switches. The proposed high step up dual switch topology [5] is shown in the figure below.

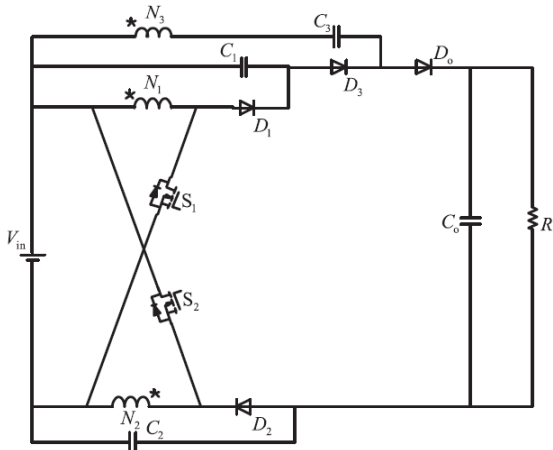


Fig. 2: Dual switch converter topology with coupled inductor

In the above figure the input DC voltage source is replaced with PVA with fluctuating voltage by variation of solar irradiation. N1, N2 and N3 [6-8] are the three windings of the coupled inductor. Switches S1 and S2 are MOSFETs connected with body diode which protects the switches from circulating currents. The resistance at the output is removed and an inverter is connected for the operation of PMSM [6]. The working of dual switch topology is elaborated by eight modes of operation.

The gain of the converter is given as $G_k = V_o/V_{in} = \frac{V_{c1}+V_{c2}+V_{c3}+V_{c4}+V_{in}}{V_{in}} \dots\dots\dots(2)$

Where, Vo is output voltage of converter, Vin is input voltage from PVA, Vc1, Vc2, Vc3, Vc4 are the voltages across the capacitors C1, C2, C3, C4 respectively.

Mode I: During this mode the switches S1 and S2 are switched ON and starts conducting. The inductor L2 along with leakage and magnetizing inductances (Lk and Lm) are charged by input source PVA. As the inductors gets charged from the input source the output capacitor Co provides charge at the output terminals.

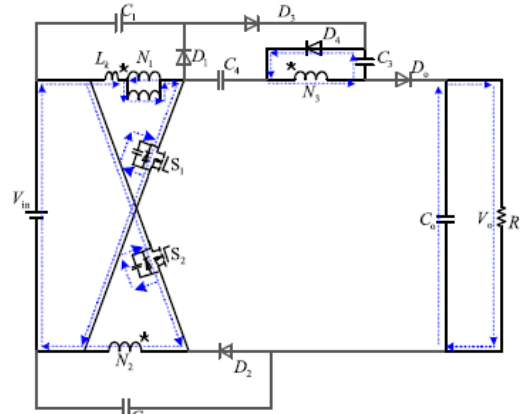


Fig. 3: Mode I current conduction

Mode II: In this interval the switches remain in ON state with only diode D3 in forward bias. The blocking capacitor C4 is now charged along with leakage and magnetizing inductances (Lk and Lm). Even in this mode, voltage at the output terminals of the converter is provided by the, Co, the output capacitor.

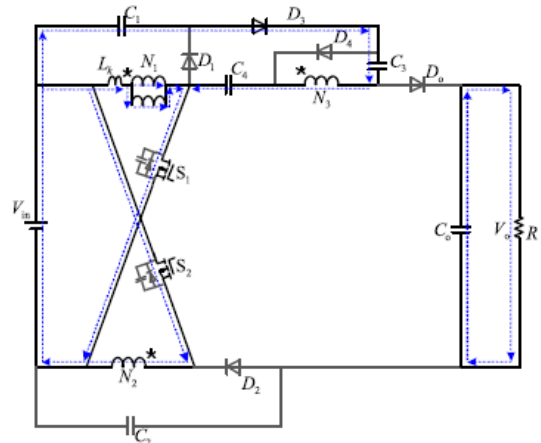


Fig. 4: Mode II current conduction

Mode III: After mode II in this mode the switches S1 and S2 are turned OFF. The energy which charged leakage and magnetizing inductances is now released into the parasitic capacitors of the switches. Even in this mode the output capacitor Co provides voltage at the output terminals of the converter.

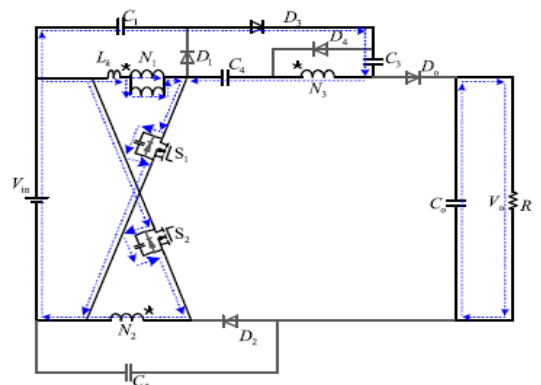


Fig. 5: Mode III current conduction

Mode IV: In this mode the switches remain in OFF state making the energies of leakage inductance L_k and magnetizing inductance L_m to release into C_1 clamping capacitor. The energy present in inductor L_2 is released into C_2 clamping capacitor. Even in this mode, voltage at the output terminals of the converter is provided by the, C_o , the output capacitor.

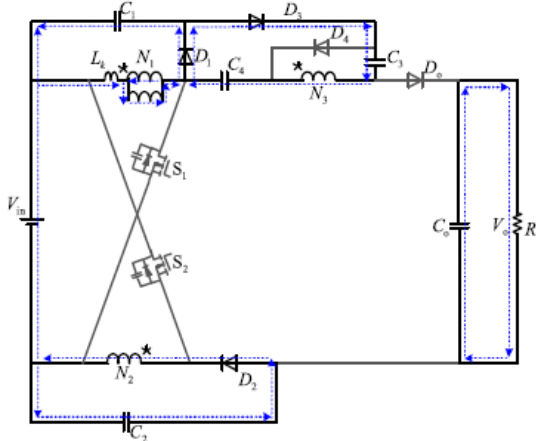


Fig. 6: Mode VI current conduction

Mode V: In this mode the switches are in OFF state and the diodes D_1 D_2 and D_o are in forward bias condition making the energies of leakage inductance L_k and magnetizing inductance L_m to release into C_1 clamping capacitor. The input PVA source, coupled inductor and capacitor C_4 are now connected in series generating a very high DC voltage. This voltage charges the output capacitor and also provides voltage at the output terminals.

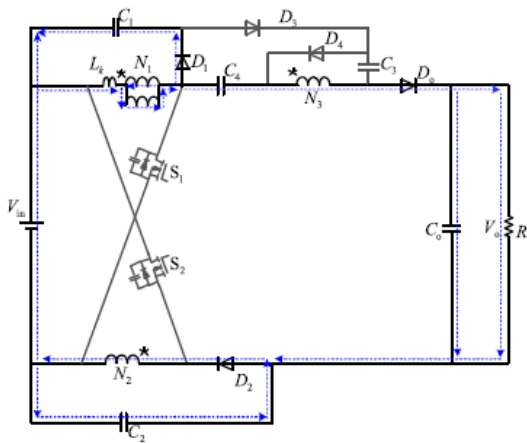


Fig. 7: Mode V current conduction

Mode VI: This mode is same as mode V with only difference of discharging of capacitor C_2 . This mode ends when D_4 diode is forward biased.

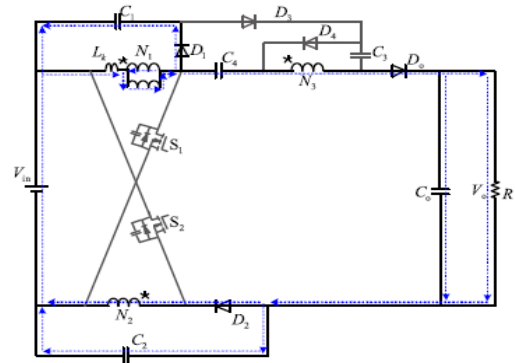


Fig. 8: Mode VI current conduction

Mode VII: The switches S_1 and S_2 still remain in OFF state with inductor L_2 and capacitor C_2 discharging into the output capacitor C_o and inverter. The inductor L_1 is also discharging providing high voltage gain at the output. A part of energy from L_2 is discharged to C_3 .

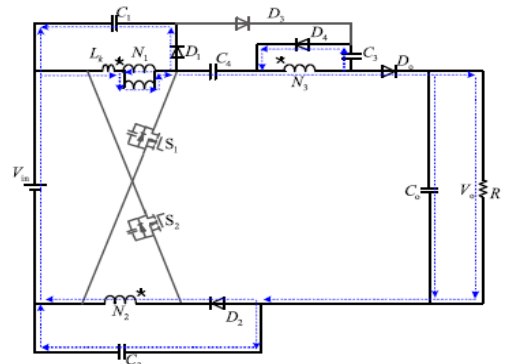


Fig. 9: Mode VII current conduction

Mode VIII: In this last mode the switches still remain OFF with D_3 and D_o in forward bias conditions. The input source PVA, leakage inductance, magnetizing inductance, capacitors C_3 and C_4 , inductor L_3 are connected in series providing very high voltage gain output charging the output capacitor C_o and providing voltage to the inverter.

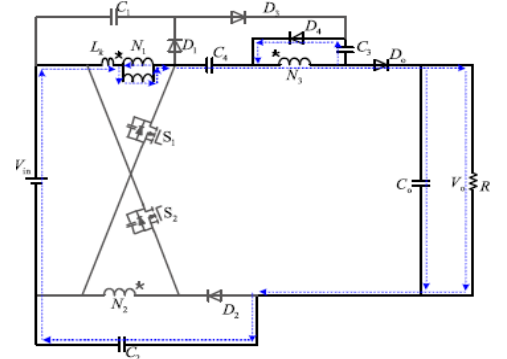


Fig. 10: Mode VIII current conduction

III. SPEED CONTROL OF PMSM

The controlled output voltage from the proposed dual switch converter is fed to six switch inverter driving a three phase PMSM [9]. The speed control of the PMSM drive is shown in the figure below. The inverter used is IGBT power electronic device six switch inverter.

Speed Control of PMSM with High Step-Up Dual Switch Solar Converter

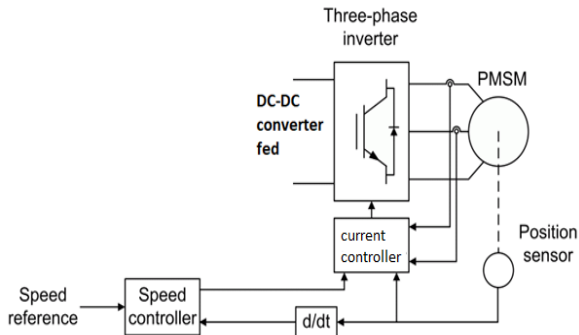


Fig. 11: Speed control of PMSM

In the above figure it can be seen that speed sensing is done which is compared to a reference speed value. The error generated is fed to PI controller generating reference electromagnetic torque T_e . The PI controller has proportional and integral gains which converts one parameter to another for generation of reference signals. The below is the PI controller block diagram with comparison of reference and measured values of speed generating reference electromagnetic torque.

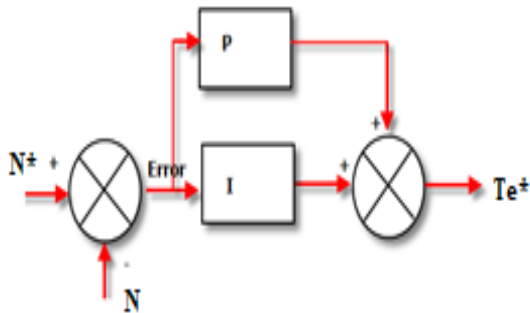


Fig. 12: PI speed controller

The torque is converted to quadrature component by the below equation

$$I_q^* = \frac{2}{3} \frac{P \lambda}{\omega} T_e^* \quad (3)$$

Where, P is number of pole pairs and λ is flux linkages in Wb.

The direct axis component is considered as zero and the rotor angle theta is multiplied with number of pole pairs for synchronization of reference signals.

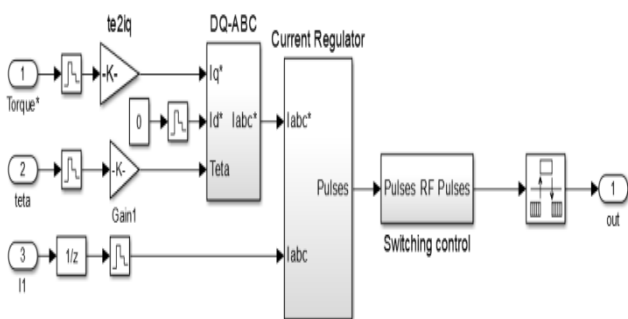


Fig. 13: Internal control structure of current control

An inverse parks transformation is applied to convert dq to abc reference signals. The reference current waveforms I_{abc}^* and measured current waveforms I_{abc} are compared, hysteresis current loop [10-13] controller is fed by this error between I_{abc}^* and I_{abc} , thus generating pulses for six switch

inverter. The hysteresis current loop controller generates pulses with respect to the error value generated by the comparison of I_{abc}^* and I_{abc} of PMSM. The below is the hysteresis current loop control for generation of pulses for IGBTs.

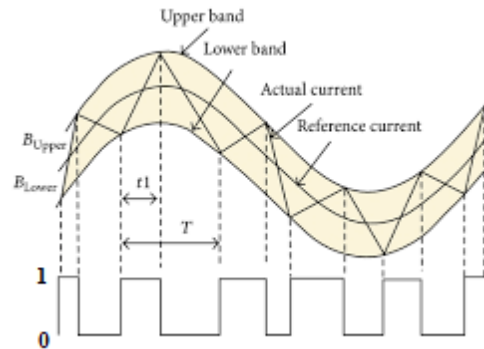


Fig. 14: Hysteresis current loop controller

The hysteresis controller has specific upper and lower bands where the value generation is done with respect to the value in the range. A low signal '0' is generated when the value is crossing upper band and a signal high '1' is generated when the value is crossing lower band. With this the current output of the inverter is controlled maintaining the speed of the PMSM even with change in mechanical torque. The rating of the PMSM is given in Table I below.

Table I

Parameter	Value
Phase resistance	0.2 ohms
Phase inductance	0.0085 H
Flux linkage	175 mWb
Inertia	89 mkg/m ²
Friction constant	5 m N-m s
Pairs of poles	4
Type of rotor	Salient pole machine

IV. SIMULINK RESULTS

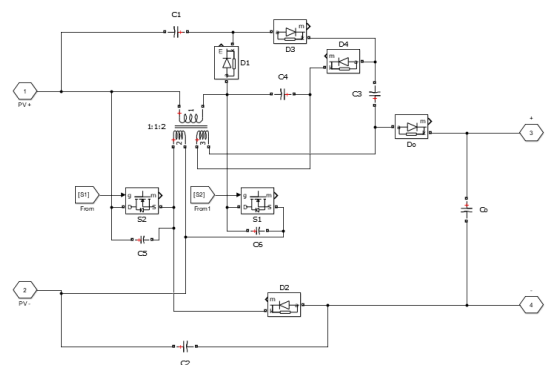


Fig. 13: Modeling of dual switch topology

The above is the MATLAB Simulink modeling of proposed converter with two MOSFETs connected. The input is a low voltage DC source and the output is stepped up DC voltage fed to six switch inverter PMSM drive.

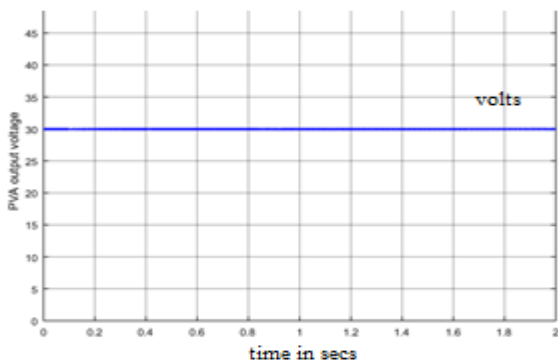


Fig. 14: PVA output voltage

The above is the graph of PVA output voltage which is at 30V and remains same till 2sec of the simulation time. This low voltage renewable source is connected to dual switch LLC resonant converter which steps up the voltage to 350V with a gain near to 10. The below is the graph of output voltage of dual switch LLC resonant converter with respect to time.

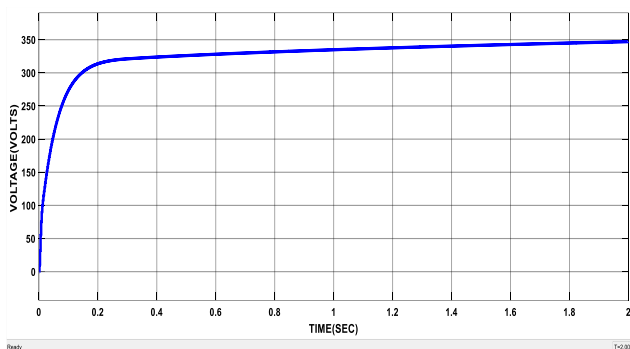


Fig. 15: Output voltage of dual switch converter

The Fig. 16 is the speed and electro-magnetic torque characteristics of PMSM with respect to time. The speed of the machine is increased from 0rpm considering it as initial state of the machine. The speed reference at initial simulation is give as 1000rpm. The speed gradually raises from 0 to 1000rpm with a rise time of 0.6sec. During the speed raise time the electromagnetic torque is at maximum and drops to rated value at 0.6sec. The comparison can be seen clearly in the graph below.

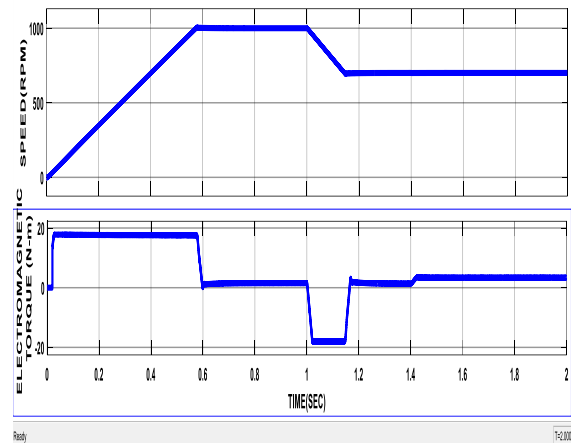


Fig. 16: Speed control of PMSM

After running the simulation for 1sec the speed reference is changed to 700rpm where the speed of the motor gradually drops to 700rpm and settles at 1.17sec, during this state the electromagnetic torque is in rated negative axis. After the speed settles to 700rpm at 1.17sec the electromagnetic torque settles back to rated value. In further modification the mechanical torque is increased from 1N-mt to 3N-mt at 1.4sec. The electromagnetic torque changes to 3N-mt maintaining the speed at reference value 700rpm.

V. CONCLUSIONS

The results showed that the output voltage of PVA is recorded at 30V and the voltage is multiplied approximately by 10 times to achieve 350V by the dual switch converter. The increased output voltage of the DC-DC converter is fed to inverter for the operation of PMSM. The speed of PMSM is considered to be 0 at initial state which increases gradually to the set value of 1000rpm. The reference speed is then reduced to 700rpm at 1sec. The speed is maintained at 700rpm even when there is change in the load torque of the PMSM. The result clearly shows that the proposed converter has good dynamic response. All the graphs are represented with respect to time.

REFERENCES

1. Altas, I. A. M. Sharaf, 2007 "A photovoltaic array (PVA) simulation model to use in Matlab Simulink GUI environment." IEEE I-4244-0632 -03/07.
2. M. Buresch, 1983, Book "PV energy syste design Mc Graw hill, New York"
3. Weidon Xiao, 2004 "A novel modeling method for photovoltaic cells" 2004, 35th annual IEEE power electronic specialist conference.
4. R. Li and D. Xu, "Parallel operation of full power converters in permanent-magnet direct-drive wind power generation system," IEEE Trans. Ind. Electron., vol. 60, no. 4, pp. 1619–1629, Apr. 2013.
5. B. Axelrod, Y. Berkovich, and A. Ioinovici, "Switched-capacitor/switched-inductor structures for getting transformerless hybrid DC-DC PWM converters," IEEE Trans. Circuits Syst. I, vol. 55, no. 2, pp. 687–696, Mar. 2008.
6. S. Lee, P. Kim, and S. Cho, "High step-up soft-switched converters using voltage multiplier cells," IEEE Trans. Power Electron., vol. 28, no. 7, pp. 3379–3387, Jul. 2013.
7. Q. Zhao and F. C. Lee, "High-efficiency, high step-up dc-dc converters," IEEE Trans. Power Electron., vol. 18, no. 1, pp. 65–73, Jan. 2003.
8. T. J. Liang and K. C. Tseng, "Analysis of integrated boost-flyback step-up converter," in Proc. IEE Electr. Power Appl., vol. 152, no. 2, pp. 217–225, Mar. 2005.

Speed Control of PMSM with High Step-Up Dual Switch Solar Converter

9. Bimal K. Bose. "Modern Power Electronic and AC Drive" Prentice Hall PTR, ISBN 0-13-016743-6, 2002.
10. Timothy L. Skvarenina., "The Power Electronics Handbook," Industrial Electronics Series, CRC Press LLC. ISBN 0-8493-7336-0, 2002.
11. Marek Jasinski, Marian P. Kazmierkowski., "Direct Power Constant Switching Frequency Control of AC/DC/AC Converter-Fed Induction Motor" Industrial Technology, IEEE International Conference on Industrial Technology (ICIT), Volume 2, 8-10 Dec, Page(s):611 – 616, 2004.
12. AnithaPaladugu and Badrul H. Chowdhury., "Sensorless Control of Inverter-Fed Induction Motor Drives" Electric Power Systems, Volume 77, Issues 5-6, April, and Pages: 619-629, Elsevier 2007.
13. S.R Bowes and D. Holliday., "Comparison of Pulse-Width-Modulation Control Strategies For Three-Phase Inverter Systems" IEE Proc. Electr. Power Appl., Volume 153, No. 4, July 2006.

AUTHORS PROFILE



University Hyderabad .

Pramod Gollapelli graduated in EEE from Vaagdevi College of Engineering affiliated to Jawaharlal Nehru technological University Hyderabad in 2015. M.Tech in Power Electronics and Electrical Drives from Anurag Group of Institutions (Autonomous), Venkatapur, Ghatkesar, Medchal Dist., Telangana State, India, affiliated to Jawaharlal Nehru Technological



Venu Madhav Gopala received his B.Tech. degree in Electrical and Electronics Engineering from Jawaharlal Nehru Technological University, Hyderabad in 2002. M.Tech. degree in Power and Industrial Drives from Jawaharlal Nehru Technological University, Anantapur in 2005. He obtained his Ph.D. from Jawaharlal Nehru Technological University, Hyderabad in 2016. He also completed Master of Business Administration (MBA) from Annamalai University in 2013. Currently he is working as Professor, Dept. of EEE, Anurag Group of Institutions. He has published several National and International Journals and Conferences and got a Patent also. He has written Text Book on "A Modified DPC Strategy for Doubly Fed Induction Generator, LAP Lambert Academic Publishers and a Full Chapter on "Rotor Flux Reference Generation Control Strategy for Direct Torque Controlled DFIG", InTech Open Publishers. He is regular Invited Faculty to Central Institute of Rural Electrification, Aram Ghar, Hyderabad for National/International Delegates. His area of interest is Advanced Control strategies of Electric Drives, Renewable Energy Technologies, Microprocessors and Microcontrollers, Fuzzy logic & ANN applications, and Network Analysis. Have professional society memberships in IEEE (M), IETE (M), ISTE (LM), IE (AM), SESI (LM), NIQR (LM), SSI (LM), SPE (LM), ISCA (LM), IAENG (LM), IACSIT (LM) and C Eng.